AAG2020
Advances in Architectural Geometry 2020
Ecole des Ponts, Univ. Gustave Eiffel
Champs-sur-Marne, France

Structural upcycling: Matching digital and natural geometry

Felix Amtsberg[1,*,†], Yijiang Huang[2,*], Daniel J.M. Marshall[2], Kevin Moreno Gata[3], Caitlin Mueller[2]

[1] Institute for Computational Design and Construction, University of Stuttgart, 70174, Germany

[2] Massachusetts Institute of Technology, Cambridge, MA 02139, USA

[3] Chair of Structures and Structural Design, RWTH Aachen University, 52062, Germany

[†] Corresponding author e-mail: felix.amtsberg@icd.uni-stuttgart.de

[*] Authors contributed equally

Abstract

This paper presents a design-to-fabrication workflow for spatial structures that make best use of a given stock of tree forks. Still little explored, the reuse of structural components beyond their traditional life cycle has the potential to significantly reduce the environmental impact of building structures. While previous work employs complex machining processes to harness the natural variation of tree forks, this work presents a new approach to optimize the use of resourced tree forks as load-bearing joints and find a matching between the intended geometry and naturally available inventory. This approach minimizes extra machine processing time by taking advantage of the structural potential of each individual tree fork that originates from its natural geometry and internal grain structure. The contributions of this paper include: (1) a digital approach for material library intake and management; (2) a geometric matching algorithm to match designed geometry and material library; (3) the development of a structural node geometry that facilitates an efficient automated fabrication process. A human-scale built prototype is presented to showcase the effectiveness of the proposed workflow, demonstrating its potential to be deployed in a practical architectural scale.

Keywords: Material upcycling, Geometric matching, Resource assignment optimization, Design-to-fabrication, Structural design

1 Introduction

1.1 Background

Timber structures have seen a resurgence in structural design in recent years due to a desire to reduce embodied carbon in the built environment. The building sector is the major contributor of over 30% of global green-house gas emissions, 40% of global energy use and 50% of global waste [United-Nations (2009)]. To reduce these building embodied impacts, timber, as a low-embodied carbon material, has been promoted as a means to shift away from the current dominant use of concrete and steel. This crucial shift to much more sustainable strategies defines new agendas on all scales. A draft bill in France requests public buildings to be constructed using 50% timber or another sustainable building material by 2022 [Bremner (2020)]. The "Holzbau-Offensive" state of Baden-Württemberg in Germany, explicitly supports timber and favors them for public buildings [Baden-Württemberg (2018)]. Supported by these new agendas and technological developments, new timber buildings appear around the globe and reach new dimensions continuously. This progress is predominantly achieved by the usage of engineered and standardized mass-timber products like glue or cross-laminated timber (GLT/CLT). While such products certainly offer value to the market, they predominantly use straight parts of high quality wood in a machine intensive production process.

Figure 1: Typical ratio between timber to be used in construction (left) and leftover material (right) of deciduous trees in a forest in Germany.

Furthermore, standardized timber construction elements are made by machine cutting, although more detailed geometric information is obtained by 3D scanning or computer tomography [Rais et al. (2017)] to guide the cutting process around natural imperfections such as knots and voids. The unique individual characteristics that were once crucial for each plant to grow and thrive are considered as downgrades and remain unused (Figure 1). This treatment of timber is clearly influenced by industrialized production of other mass-construction materials like concrete or steel. However, this "mass-production" approach does not utilize the individual strengths of natural construction materials, related to organic geometries and internal fiber orientation, and thus calls for alternative, more effective solutions (Figure 2).

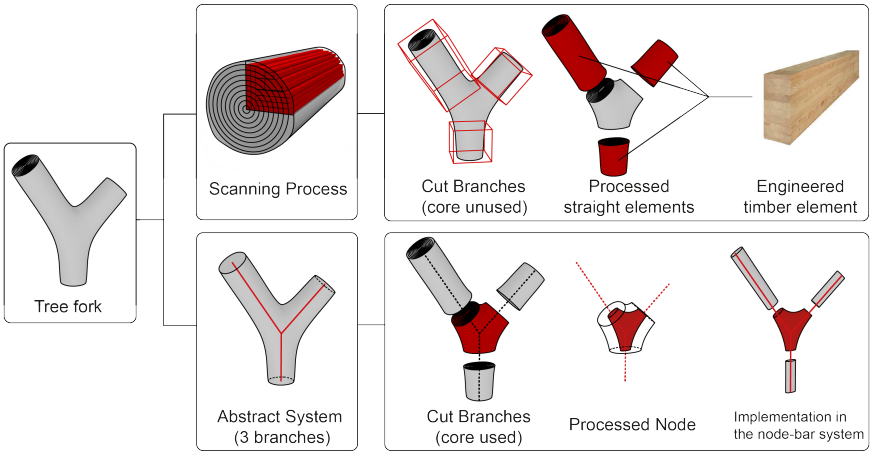

Figure 2: While state-of-the-art scan-to-fabrication processes identify defects and optimize cutting sequences for linear homogeneous elements, "structural upcycling" uses the information to add value to otherwise potentially discarded parts.

This paper proposes a novel design-to-fabrication workflow which uses tree forks, typically cut, removed, and chipped in the harvesting process. Despite this convention, tree forks are actually highly efficient structural components that incorporate high-strength fibers linked together in complex 3D branching geometries; human manufacturing processes are not yet capable of replicating the intelligent material programming inherent in these abundant natural resources. This research therefore seeks to make structural use of tree forks as efficient 3D joints for spatial structures. In the workflow presented in this paper, these tree branches are collected, digitally archived, computationally matched to the design geometry, and optimized for achieving higher matching score. Then, robotic processing technique is employed to process the tree branches efficiently.

In this method, naturally available under-utilized resources, shaped by the conditions in their environment, are given increased value. For example, the timber forks used to build the prototype presented in this paper come from felled urban street trees that would otherwise be chipped. The digital design process for building with available resources opens up the potential for structurally efficient resource consumption and a new design philosophy.

1.2 Related work

Material availability-informed design processes have shown high potential not only in developing novel design concepts, but also giving increased value to underused material. Recent studies have shown that many of these materials, if collected carefully, can be recovered and reintegrated in the construction workflow of new structures and buildings, providing both environmental and economical incentives [Arora et al. (2020)]. However, this design strategy involves reversing the conventional structural design process, because the synthesis of a structural layout (geometry and topology) is constrained by mechanical and geometric properties of

an available stock of elements [Gorgolewski (2008)].

Computational exploration of material availability constrained design has received limited attention but is of increasing interest in the literature. Existing work has focused on structural optimization of linear elements' cross section or topology with a stock constraint on the elements (defined by length and cross section). The optimization of plane frames of fixed topology from a stock of onetime available cross sections is presented in [Fujitani and Fujii (2000)]. Bin-packing strategies are used to form-fit a stock of wood logs to statically determinate trusses in [Bukauskas et al. (2017)]. Recently, mixed-integer programming is proposed to solve stock constrained topology optimization problems for spatial trusses [Brütting et al. (2019)]. It is noteworthy that most of this previous work focuses on reusing linear steel or wood structural elements. The optimized design might require *complex joint connections*, which requires extra fabrication efforts and cost. This paper complements previous research by specifically investigating the structural potential built in the natural geometry of the tree forks and uses these forks directly as structural joints, thus circumventing extra fabrication cost of joint making.

Other studies have explored incorporating natural materials into design without processing them into a standardized form. In [Self and Vercruysse (2017)], tree forks are scanned and used in an almost unprocessed form to build a large-scale pavilion, but does not formalize a generalized design strategy to incorporate design intent. [Von Buelow et al. (2018)] employs delicate but time-consuming machining operations to process the tree fork into desired shapes. In contrast, instead of investing significant time in converting the natural geometry to fit into a geometrically incompatible design, this work aims to find a compromise between the resources and the design. Structural efficiency is obtained by following the individual geometry of each unique tree fork and its internal fiber orientation, without forcing them to "comply" to an unmatched structural intent (Figure 2).

Finally, it is worth noting that the computational approach used in this work draws some conceptual mathematical similarity with the surface panelization problem [Huard et al. (2015)], where a smooth surface is approximated by a nearly smooth union of discrete panels of a minimal number of types. Although both approaches adapt an alternating discrete-continuous optimization procedure [Eigensatz et al. (2010)], the presented work is constrained with a given set of material inventory and thus requires a completely different solving technique.

2 Methodology

2.1 Overview

This section introduces the computational design and fabrication process for working with an inventory of tree forks to create discrete spatial structures (e.g. grid shells, trusses, space frames, etc. composed of linear elements and structural nodes or joints). The proposed design workflow matches the recycled tree forks to their optimal placement as structural nodes on the design, and uses externally sourced off-the-shelf standard elements as the linear structural elements. While the method

is intended to be general, in order to explain it with specificity, the prototype structures introduced in Section 2.5 is sometimes referenced in the description below.

The overall design-to-fabrication process is divided into 5 steps (Figure 3):

1. The tree forks collected are cut to a length of 10 to 30cm per fork. A digital scanning is performed upon each fork and these geometric information is gathered together to form a digital material library (Section 2.2).
2. With a given initial design of the structure, the geometric information of tree forks are used to match them with structural nodes on an target design, find the best fitting fork for the joint and generate the node geometry (Section 2.3).
3. By incorporating the quantitative matching score into an optimization process and parameterized design space, an optimized design can be obtained that balances the trade-offs between resource matching, design intent approximation, and structural performance (Section 2.5).
4. The geometry of each structural node is used to automatically generate the machine code for fast robotic band saw cutting (Section 2.6).
5. Finally, these processed structural nodes, combined with externally sourced standard linear elements, can be assembled on site to construct the structures.

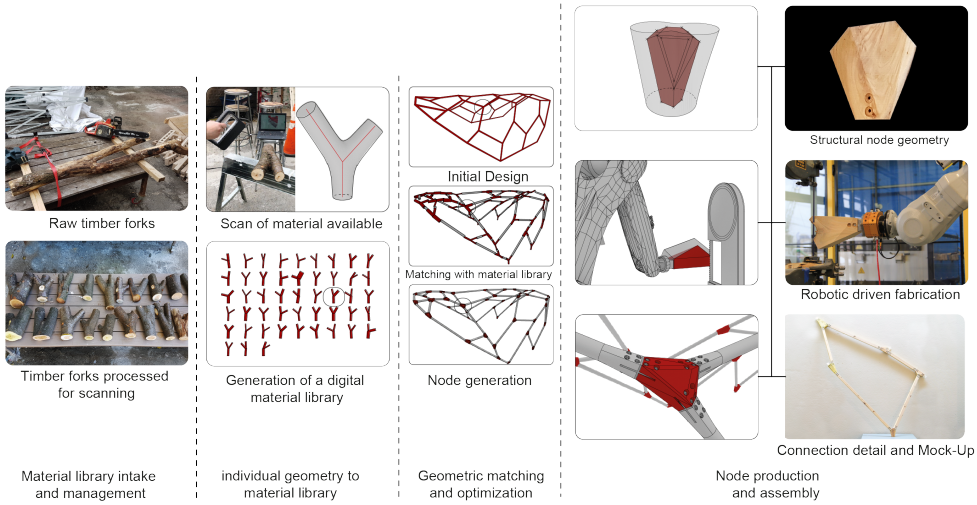

Figure 3: Design-to-fabrication process overview.

2.2 Material library intake and management

The process starts with an analysis of the geometric properties of the intake tree forks. Trees appear in various species, and provide a huge diversity in terms of geometric and material properties [Hoadley (2000)]. The use of structural timber is dominated by softwood, coming from *coniferous* wood like spruce and Douglas fir,

among others. However, tree forks from a broader range of species of deciduous trees are of interest in this work, because they typically have more relevant branching geometries and element diameters, and because they are widely available in urban forests (e.g. street trees). For example, the prototype introduced later uses forks from deciduous urban trees in the locale of the authors.

Even though the sources are from different species from different locations, three-branched forks, like the ones used in this research, are geometrically similar. The typical branching behavior of deciduous trees is a 3-valence Y-shaped branching, where the section area of the lower branch is approximately the area of the two upper branches combined [Rodewald and Schlichting (1988)].

The tree forks in this research can therefore be abstracted with three-element bar assemblies connected at a point, which represent a skeletonized version of the tree branch fork (Figure 4). The primary structural information of interest is the relative geometry/orientation of the branches, expressed as three unit vectors, since this dictates the internal fiber orientation that gives the component its strength. Element diameter is also important both for structural capacity calculation and fabrication planning, and can also be stored in this representation.

To convert the physical tree fork inventory into a digital library in this format, a variety of photogrammetry technologies are available. For the prototype in this paper, simple consumer-grade 3D scanners were used to obtain 3D mesh geometries of the fork surfaces, and the vector and radius information was manually extracted from these meshes. More sophisticated techniques with better imaging and automation could be explored in the future.

Figure 4: Collection of Y-shaped branches and their combined geometric range (top view and side view)

2.3 Matching the design and material library

To link the design and the obtained material library, each of the three-valence nodes in the design geometry needs to be matched with a best-fit tree fork in the material library. There are two main technical difficulties that need to be resolved here: (1) defining a metric to quantify the mismatch error between a three-valence node on the design geometry and a tree fork; (2) designing a computational algorithm to find the optimal matching that minimizes the overall accumulated mismatch error based on the proposed metric.

In this project, the mismatch metric is measured by geometry alignment and computed by a simplified Iterative Closest Point (ICP) algorithm [Besl and McKay (1992)] (Section 2.3.2). The minimal weight matching is solved by the Hungarian assignment algorithm (Section 2.3.3). Figure 5 shows an overview for the geometric matching workflow.

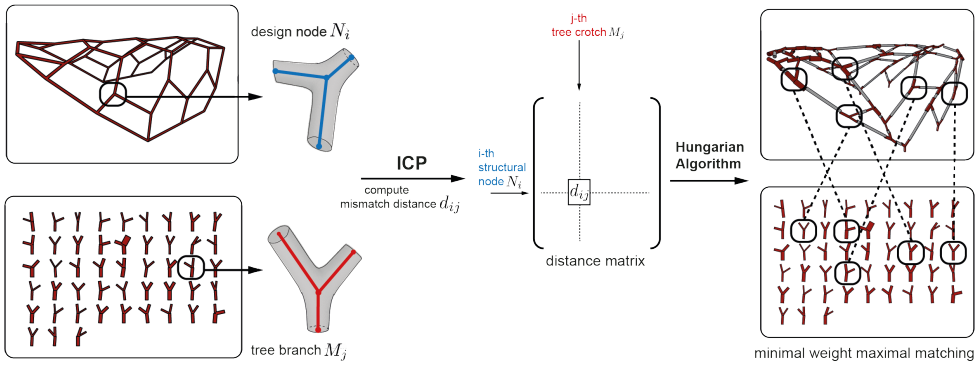

Figure 5: The geometry and material library matching workflow.

2.3.1 Matching problem formulation

Assuming that the target design has n three-valence structural nodes $\mathcal{N} = \{N_i | i \in \{1, \cdots, n\}\}$ and the material library has m tree forks $\mathcal{M} = \{M_j | j \in \{1, \cdots, m\}\}, m \geq n$, an ideal matching finds a map $C : \mathcal{N} \to \mathcal{M}$ such that:

1. C is injective, i.e. $C(N_i) \neq C(N_j)$, if $i \neq j$.
2. C minimizes the overall mismatch between $\mathcal{M}$ and $\mathcal{N}$.

Notice that equivalently, the map can be written as a map on the index set: $C : [n] := \{1, \cdots, n\} \to [m] := \{1, \cdots, m\}$. It's implicitly assumed that $m \geq n$, i.e. enough resource exists in the material library to build the target design.

Then, if a notion of metric $d(\cdot, \cdot)$ is defined to measure the mismatch between any N_i and M_j, the matching problem can be formulated as:

$$\min_{C:[n]\to[m]} s(C) = \sum_{i=1}^{n} d(N_i, M_{C(i)}) \tag{1}$$

which is a minimum-weight linear assignment problem, a fundamental and well-understood combinatorial optimization problem on weighted bipartite graph [Bertsekas (1998)]. In this work, the objective function $s(C)$ is called the *global matching score*. It can be solved exactly in polynomial time, e.g. by using the Hungarian algorithm [Kuhn (1955)].

However, the mismatch metric $d(\cdot, \cdot)$ in Equation (1) needs to be designed carefully. Its design and computation is described in the next section.

2.3.2 *Mismatch metric*

Given a design node $N \in \mathcal{N}$ and a tree fork $M \in \mathcal{M}$, a well defined metric $d(\cdot,\cdot)$ needs to satisfy the following properties:

1. The metric d must be non-negative and symmetric, i.e. $d(M,N) = d(N,M) \geq 0, \forall N \in \mathcal{N}, M \in \mathcal{M}$.
2. The metric must be invariant to rigid-body transformation, i.e. rotation, translation, reflection and their combinations (Figure 6).

The second property above is essential. Every design node and tree fork has its own coordinate frame, which means simply computing distance from each point $u \in M$ to its closest point $v \in N$ and summing the squared distances will not yield a rigid-body transformation-invariant distance.

As discussed in Section 2.2, each tree fork is represented by its central line skeleton (Figure 6). The four end points of the skeleton line segments is used as a compact representation of the central lines: $N_i = \{u_0^i, u_1^i, u_2^i, u_3^i\}$ and $M_i = \{v_0^i, v_1^i, v_2^i, v_3^i\}$, where u_0^i and v_0^i denotes the central points that have valence three. The central points (u_0^i and v_0^i) are always matched together to make sure the structral working point of the tree fork coincides with the one indicated in the target design. In an ideal match, the internal fiber structure of the fork is completely aligned with the axis of the connecting structural element, resulting in a maximal use of the inherent strength of the wood fiber. As mismatch increases, the strength of the structural connection is degraded nonlinearly (e.g. strength degrades rapidly once mismatch exceeds around 10 degrees). Hankinson's Equation [Hankinson (1921)] describes this relationship of timber strength and fiber orientation. Based on this, the intuition of this paper is that a perfect match allows for the most structurally efficient use of the available fork material library. Future work could encode the Hankinson's Equation relationship more explicitly in the matching quantification.

Properties 1 and 2 of a well-defined mismatch distance above call for a joint optimization of rotation, translation, and skeleton line end points correspondence. Thus, the mismatch metric computation problem can be formulated as matching two point sets with size three:

$$\begin{aligned} & d(N,M) := \min_{R,t,c} \sum_{i=1}^{3} \| R \cdot u_i^N + t - v_{c_i}^M \|_2^2 \\ s.t. \quad & R^T = R^{-1}, R \in \mathbb{R}^{3\times 3} \\ & t \in \mathbb{R}^3 \end{aligned} \tag{2}$$

where $u_i^N, v_i^M \in \mathbb{R}^3$ are the target design node N and the tree fork M's skeleton line's valence-one end points, respectively. The decision variable c_i is the integer index of the point in M that corresponds most closely with the i-th point in N. The decision variable $R \in \mathbb{R}^{3\times 3}, t \in \mathbb{R}^3$ are the rotation matrix and translation vector,

respectively. The constraint in R in eq. 2 forces the matrix R to be orthogonal. This formulation is widely used in solving the point cloud registration problem (e.g. in [Besl and McKay (1992)]).

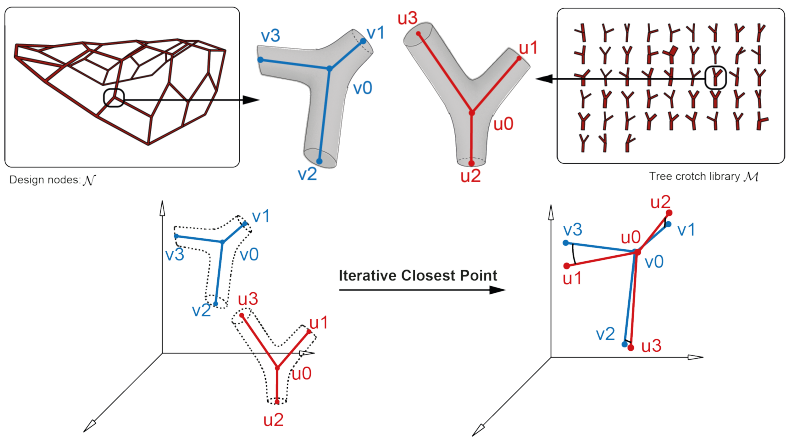

Figure 6: Computing the mismatch distance between a design node $N \in \mathcal{N}$ and tree fork $M \in \mathcal{M}$ by using a simplified ICP algorithm.

In this paper, this point registration problem is solved by computing the optimal alignment R and t for all six possible point correspondence, and selecting the one with lowest mismatch error. When solving for the optimal rigid motion R and t, the algorithm utilizes the fact that if a correspondence between two point clouds is given, R and t can be calculated in close form (e.g. the analytical solution to the orthogonal Procrustes problem) [Sorkine-Hornung and Rabinovich (2017)]:

Theorem: Let $X' := \{x_i - \bar{x} | i \in [n]\} = \{x'_i\}, Y' := \{y_i - \bar{y} | i \in [n]\} = \{y'_i\}$ where $\bar{x} = \frac{1}{n}\sum_{i=1}^{n} x_i$ and $\bar{y} = \frac{1}{n}\sum_{i=1}^{n} y_i$ denotes the center of masses. Let the 3×3 covariance matrix $S = \tilde{X}\tilde{Y}^T$, $\tilde{X}$ and $\tilde{Y}$ are the $3 \times n$ matrices that have x'_i and y'_i as their columns. The SVD decomposition of S is denoted by $S = U\Sigma V^T$, where $U, V \in \mathbb{R}^{3\times 3}$ are unitary, and Σ is a diagonal matrix with singular value of S as its diagonal. Then, the optimal solution of $E(R,t) = \frac{1}{n}\sum_{i=1}^{n} \|R \cdot x_i + t - y_i\|^2$ is unique and is given by:

$$R^* = V \begin{pmatrix} 1 & 0 & 0 \\ 0 & 1 & 0 \\ 0 & 0 & det(VU^T) \end{pmatrix} U^T$$
$$t^* = \bar{y} - R^* \cdot \bar{x} \tag{3}$$

2.3.3 Solving the global matching problem

Now that a metric $d(\cdot,\cdot)$ is defined to measure the mismatch error between a pair of tree fork and a structural node, a mismatch distance matrix $D \in \mathbb{R}^{n\times m}$ can be constructed by having $D_{ij} = d(N_i, M_j)$. Then, any matching optimization

algorithm that can solve the minimal-weight linear assignment problem can be employed. The chosen matching algorithm takes the distance matrix D as an input and outputs the optimal match C^* (Figure 5). The optimal objective value $s(C^*)$ in Equation (1) is used as the global matching score (henceforth called *matching score*) to quantify the given geometry's material upcycling performance.

In this work, the Hungarian algorithm [Kuhn (1955)] is used for the sake of simplicity. However, for very large problem instances, other more scalable algorithms might need be used to solve the global matching problem exactly [Bertsekas (1988)] or approximately [Naiem and El-Beltagy (2013)].

2.4 Design concept and computational experiments

For this paper, the simplified ICP algorithm for computing the mismatch error is implemented in C# and an existing open-source C# implementation of the Hungarian algorithm [Vivet (2020)] is used in the environment of Rhino and Grasshopper for design exploration. From this, the matching score $s(C^*)$ can be calculated in the Rhino/Grasshopper environment by summing across the individual mismatch error $d(N_i, M_{C^*(i)})$ for the structure.

To relate the resourced material library described in Section 2.2 and the geometric matching mechanism described in Section 2.3, a desired design system would have reasonable amount of design variables to offer sufficient design variety while taking advantage of the natural strengths of the collected forks. Because the Y-shaped forks come from cantilevering branches on trees, they have moment stiffness to work as rigid frame joints in a node-bar system. They can work as structural connections that transfer bending and shear in addition to normal forces in spatial trusses or grid shells with small curvature, generated for example based on Voronoi- or honeycomb-patterns. These structural systems require bending-resistant structural nodes that have compatible valence with the tree forks.

A large number of computational experiments related to this design concept were conducted and presented in [Desai (2020)], an example of which is shown in Figure 7. In this case, a hexagonal-based grid shell is parameterized in terms of global geometry of the shell surface, and then optimized with a gradient-based algorithm to minimize the matching score of a simulated tree fork library. It is evident in the figure that the geometry of the best-match grid shell can vary significantly in response to the material library. It is also evident that the matching score improves as the number of forks in the material library increases. In general, it was found that the matching score converged when approximately three times as many forks were in the library compared nodes in the target design.

2.5 Multi-objective framework and optimization

This section presents a more detailed design method that follows a similar approach to the experiments summarized in Section 2.4. There are three key quantitative objectives to consider in this design process: (1) matching performance in reference to the material library, (2) structural performance, and (3) fidelity to the design

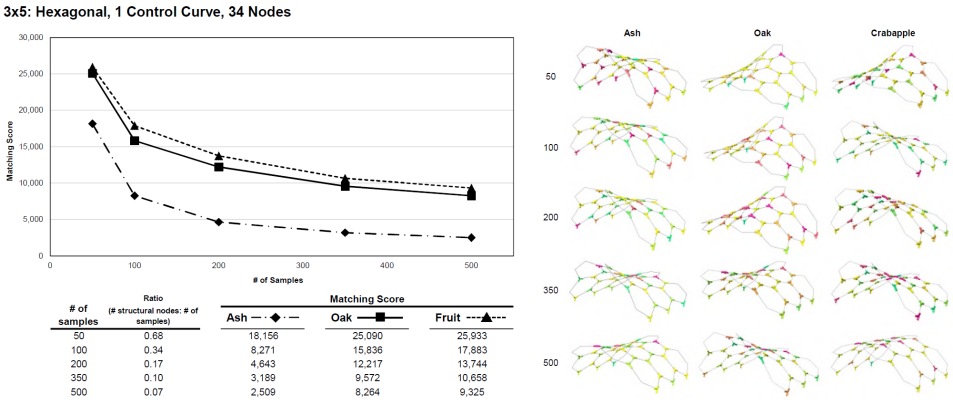

# of samples	Ratio (# structural nodes: # of samples)	Matching Score: Ash	Oak	Fruit
50	0.68	18,156	25,090	25,933
100	0.34	8,271	15,836	17,883
200	0.17	4,643	12,217	13,744
350	0.10	3,189	9,572	10,658
500	0.07	2,509	8,264	9,325

Figure 7: An excerpt from [Desai (2020)], showing the relationship between matching score, optimized geometry, and available tree forks across three different species.

intent. While it is possible to formulate the design process as a multi-objective optimization problem responsive to these three goals (e.g. as in [Brown et al. (2020)]), in this case it is perhaps more expedient to use a single-objective solver in combination with a well-considered design space.

This is possible because the first two goals of matching and structural performance can be considered identical; a perfect match maintains the best potential for structural load transfer and utilization of material, because the geometric alignment confers an internal grain structure parallel to the primary flow of forces, as discussed in Section 2.3.2. Additional structural properties of the entire structure, such as stiffness, could also be considered, but in this paper they are observed as soft constraints rather than incorporated as design drivers. The third goal of fidelity to design intent is one with multiple philosophical interpretations (e.g. in [Cuvilliers (2020)]), but here an approach that constrains the design space to options that are acceptable and of interest to the designer is used. Thus, a single-objective gradient-based solver can be used to find designs that minimize the matching score, perform well structurally, and relate to the intent of the human designer.

A specific step-by-step overview of this design worflow is given as follows:

1. An initial grid shell design is given, constructed by projecting a 2D edge connectivity pattern onto a guiding surface.

2. The central line skeleton of each node is extracted to form the structural node set $\mathcal{N}$. The mismatch distance Matrix D is then computed by using the procedure described in Section 2.3.2 comparing each $N \in \mathcal{N}$ and tree fork $M \in \mathcal{M}$. Taking the distance matrix D as an input, the Hungarian algorithm finds the optimal fork-to-node assignment together with a matching score (Equation (1)), which can be used as an objective function to direct an optimization in a parameterized design space. Notice that this process of compiling a mismatch matrix D and computing the globally optimal matching

needs to be done every time the design geometry is changed.

3. Kangaroo2 [Piker (2017)] is used as a specialized parameterization tool to enable global morphing the geometry with a small number of parameters (e.g. bar rest length, attraction curve, etc.), which are linked as variables to an optimizer (Radical from the Design Space Exploration suite [Brown et al. (2020)]).
4. The structural analysis software Karamba3D [Karamba3D (2020)] is used to check the deflections and strain energy of the final structure.

Figure 8 showcases a variety of design alternatives in the design space with varying matching scores. The space can be explored manually by tuning a small number of parameters in addition to using a numerical optimizer to arrive at a final design.

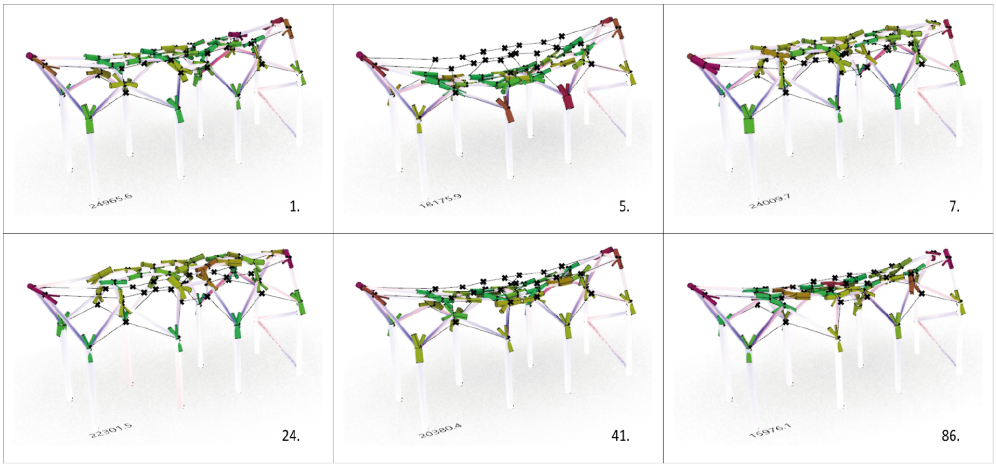

Figure 8: (1) An initial design concept with a matching score of 24965.6, after (5, 7, 24, 41) optimization iterations the matching cost reaches down to 15976.1, but deviating far from the design intent. Version (86) shows that a satisfactory result can be obtained, balancing design intention and the matching score.

Using this method, design studies were conducted based on the concept to renovate a shelter in the authors' local community. The tree forks used for the structure were resourced from the yearly demolishing process of some dangerous but yet structurally functional urban trees. The eventual aim is to bring the removed trees back and re-install them in form of a new functional structure, which recreates the atmosphere and spatial experience previously provided by the felled trees.

2.6 Design and fabrication of structural nodes and prototype

In order to verify the physical feasibility of the proposed workflow, details on the structural node are designed, together with an efficient, automated machining process. As mentioned in Section 1.2, this work puts a special focus on production efficiency and aims to avoid time-consuming, complex machining processes. This section describes some detailed design and fabrication strategies to merge material and geometrical individuality and production efficiency.

While an unprocessed tree fork shows the highest structural performance (since no material is removed) and 3 cuts would be sufficient to expose the nodes' contact faces for connections with the linear elements, the emerging geometry would complicate the handling, assembly and maintenance of the structure. An unprocessed fork resists a smooth transition between the node and the standard linear elements, and the remaining bark can lead to rot and fire hazard.

To address these issues, the convex hull covering the scanned point cloud of a tree fork is proposed as the node geometry. With this convex hull representation, acute and obtuse dihedral angles between adjacent faces caused by local concave geometric features do not appear. Thus, each convex hull can be machine-processed with a sequence of continuous linear saw cuts. Furthermore, it roughly represents the natural geometry of a tree fork, and enables a straightforward resolution of the deviation between intended digital and the provided natural geometry of the corresponding fork (Figure 9).

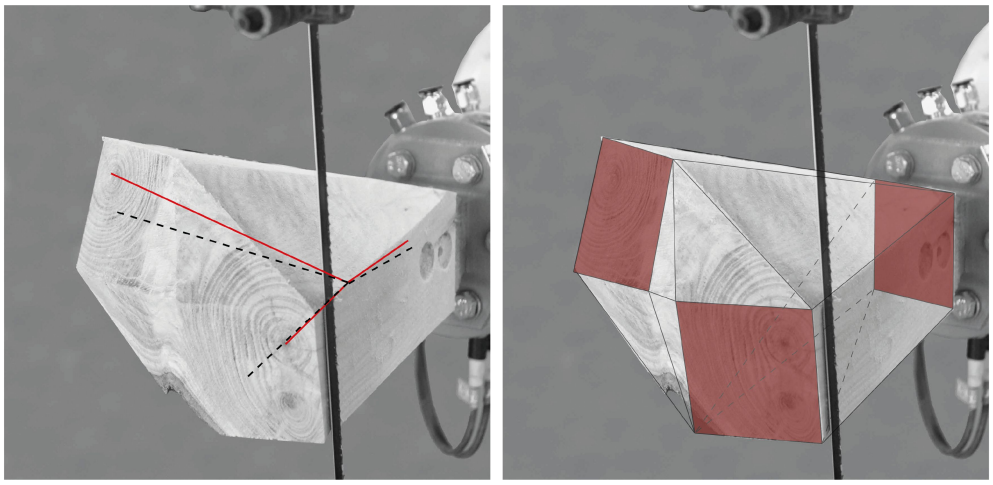

Figure 9: The Skeleton line (red) representing the tree fork and the structural node on the intended geometry (dashed line) which generates the 3 contact faces to define the convex hull.

After the matching and the optimization processes in Section 2.5 determine the final geometry of the structure and the corresponding tree forks used, the vectors of each structural node are extracted to help construct the physical node geometry. The areas of the contact faces could be informed by structural analysis and match sizing requirements by allowing bars with various cross-sectional areas to connect to the node, although for this paper's prototype a single cross section was used for simplicity. The automated algorithm for generating the final convex hull node geometry requires four pieces of input information:

- The three vectors of the corresponding structural node
- The four corner points of each of the contact faces that connect the node to a linear element

- The boundary representation of the corresponding fork geometry
- Other construction joint details (i.e. bolts, nuts, connector plates, etc.)

Using this information, the original fork geometry is computationally translated into a convex hull composed of planar quadrilateral and triangular faces (approximately 12 to 25 in total), using a custom Grasshopper script developed by the authors (see Figure 10). These faces are used to automatically design and generate the toolpath for the robotic production. Toolpath complexity is reduced to a maximum of 25 cuts to fabricate the node, which enables a simple and reliable generation of efficient toolpaths and quick machining of the nodes.

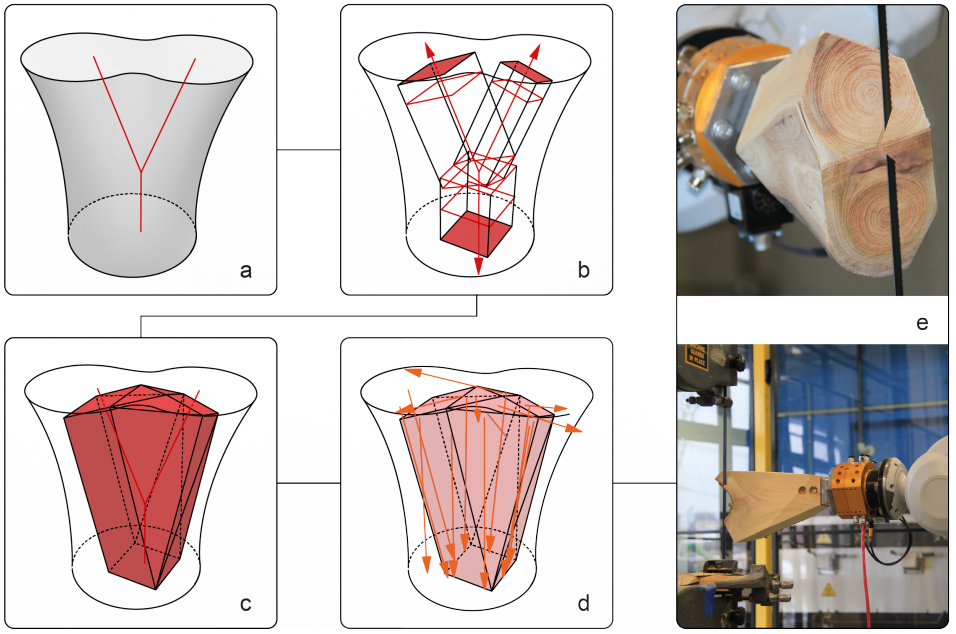

Figure 10: (a) A 3D-scan and the corresponding fork vectors. (b-c) automatic convex hull generation. (d-e) tool path for effective fabrication using an industrial robot and a stationary bandsaw.

Using this method, a demonstrator prototype was produced and temporarily installed on the campus of MIT (Figure 11). This structure had 12 nodes that were designed and fabricated using the process described above. The authors plan to install a larger version of this prototype with approximately 40 nodes to be used as an outdoor pavilion in the future.

3 Conclusion and Outlook

Today's climate crisis demands that architects and engineers develop more sustainable approaches to better utilize construction resources. This work demonstrates how the individual analysis of previously under-valued material can open up new design potentials for structurally efficient material consumption.

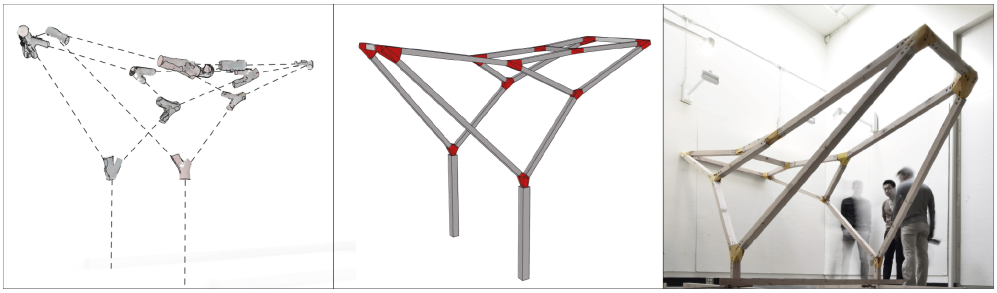

Figure 11: Matched forks, corresponding structural node convex hull geometries, and the realized prototype.

By interleaving material library management, geometric matching, and efficient machining process, the proposed computational design-to-fabrication workflow offers high degrees of design freedom, while using quantitative material availability and structural performance as guiding principles. This project comprehensively covers a new connection between natural-grown construction material, structural design, and digital fabrication.

As described above, a permanent structure at the authors' local neighborhood is under planning, where the harvested trees are brought back to their urban environment and re-installed as a new functional structure. Future research will work with larger material libraries to include multi-branch forks and intends to replace 3D-scanning with CT-scanning technologies to automatically obtain a more detailed geometric representation of the tree forks, such as precise fibre orientation, density, etc.

Further research is needed to develop a detailed understanding of the influence of grain direction on the structural capacity of the nodes, to quantify this deviation-to-decrease ratio. Finally, obtaining a shape gradient with respect to the matching score can shed light on how to incorporate combinatorial objectives into the prevailing continuous parametrized design and optimization workflow.

References

Arora, M., F. Raspall, L. Cheah, and A. Silva (2020). Buildings and the circular economy: Estimating urban mining, recovery and reuse potential of building components. *Resources, Conservation and Recycling 154*, 104581.

Baden-Württemberg, M. (2018). *Die Gestalt von Bäumen — zufällig oder gesetzmäßig?* Ministerium für Ländlichen Raum und Verbraucherschutz.

Bertsekas, D. P. (1988). The auction algorithm: A distributed relaxation method for the assignment problem. *Annals of operations research 14*(1), 105–123.

Bertsekas, D. P. (1998). *Network optimization: continuous and discrete models*. Athena Scientific Belmont.

Besl, P. J. and N. D. McKay (1992, Feb). A method for registration of 3-d shapes. *14*, 239–256.

Bremner, C. (2020). Macron: Use more wood in our buildings.

Brown, N., J. Violetta, and C. Mueller (2020). Implementing data-driven parametric building design with a flexible toolbox. *Automation in Construction , In press*.

Brütting, J., J. Desruelle, G. Senatore, and C. Fivet (2019). Design of truss structures through reuse. In *Structures*, Volume 18, pp. 128–137. Elsevier.

Bukauskas, A., P. Shepherd, P. Walker, B. Sharma, and J. Bregulla (2017). Form-fitting strategies for diversity-tolerant design. In *Proceedings of IASS Annual Symposia*, Volume 2017, pp. 1–10. International Association for Shell and Spatial Structures (IASS).

Cuvilliers, P. (2020). *The constrained geometry of structures: Optimization methods for inverse form-finding design*. Ph. D. thesis, Massachusetts Institute of Technology.

Desai, I. (2020). Designing structures with tree forks: Mechanical characterization and generalized computational design approach. Master's thesis, Massachusetts Institute of Technology.

Eigensatz, M., M. Kilian, A. Schiftner, N. J. Mitra, H. Pottmann, and M. Pauly (2010). Paneling architectural freeform surfaces. In *ACM SIGGRAPH 2010 papers*, pp. 1–10.

Fujitani, Y. and D. Fujii (2000). Optimum structural design of steel plane frame under the limited stocks of members. In *Proceedings of the RILEM/CIB/ISO International Symposium, Integrated Life-Cycle Design of Materials and Structures*, pp. 198–202.

Gorgolewski, M. (2008). Designing with reused building components: some challenges. *Building Research & Information 36*(2), 175–188.

Hankinson, R. (1921). Investigation of crushing strength of spruce at varying angles of grain. *Air service information circular 3*(259), 130.

Hoadley, R. B. (2000). *Understanding wood: a craftsman's guide to wood technology*. Taunton press.

Huard, M., M. Eigensatz, and P. Bompas (2015). Planar panelization with extreme repetition. In P. Block, J. Knippers, N. J. Mitra, and W. Wang (Eds.), *Advances in Architectural Geometry 2014*, pp. 259–279. Springer International Publishing.

Karamba3D (2020). Karamba3d: a parametric structural engineering tool. `https://www.karamba3d.com/`.

Kuhn, H. W. (1955). The hungarian method for the assignment problem. *Naval research logistics quarterly 2*(1-2), 83–97.

Naiem, A. and M. El-Beltagy (2013). On the optimality and speed of the deep greedy switching algorithm for linear assignment problems. In *2013 IEEE International Symposium on Parallel & Distributed Processing, Workshops and Phd Forum*, pp. 1828–1837. IEEE.

Piker, D. (2017). Kangaroo physics version 2.42. `https://www.food4rhino.com/app/kangaroo-physics`.

Rais, A., E. Ursella, E. Vicario, and F. Giudiceandrea (2017). The use of the first industrial x-ray ct scanner increases the lumber recovery value: case study on visually strength-graded douglas-fir timber. *Annals of forest science 74*(2), 28.

Rodewald, B. and H. J. Schlichting (1988). Die gestalt von bäumen — zufällig oder gesetzmäßig? *Praxis der Naturwissenschaften- Physik 37,5*(7), 7–12.

Self, M. and E. Vercruysse (2017). Infinite variations, radical strategies. In *Fabricate 2017 conference proceedings. UCL Press, London*, pp. 30–35. JSTOR.

Sorkine-Hornung, O. and M. Rabinovich (2017). Least-squares rigid motion using svd. Technical report, ETH Zurich.

United-Nations (2009). Buildings and climate change: Summary for decision makers. `https://www.unglobalcompact.org/`.

Vivet, M. (2020). C# implementation of the hungarian algorithm. `https://github.com/vivet/HungarianAlgorithm`.

Von Buelow, P., O. Oliyan Torghabehi, S. Mankouche, and K. Vliet (2018). Combining parametric form generation and design exploration to produce a wooden reticulated shell using natural tree crotches. In *Proceedings of IASS Annual Symposia*, Volume 2018, pp. 1–8. International Association for Shell and Spatial Structures (IASS).